https://doi.org/10.5194/acp-2019-583
Preprint. Discussion started: 25 June 2019

Atmospheric Chemistry and Physics Discussions

Contrasting ambient fine particles hygroscopicity derived by HTDMA and HR-AMS measurements between summer and winter in urban Beijing

Xinxin Fan[1], Fang Zhang[1*], Lu Chen[1], Don Collins[2], Weiqi Xu[3, 4], Xiaoai Jin[1], Jingye Ren[1],Yuying Wang[1, 5], Hao Wu[1], Shangze Li[1], Yele Sun[3, 4], Zhanqing Li[1, 6]

[1]*State Key Laboratory of Earth Surface Processes and Resource Ecology, College of Global Change and Earth System Science, Beijing Normal University, Beijing 100875, China*
[2]*Department of Chemical and Environmental Engineering, University of California Riverside, Riverside, California, USA*
[3]*State Key Laboratory of Atmospheric Boundary Layer Physics and Atmospheric Chemistry, Institute of Atmospheric Physics, Chinese Academy of Sciences, Beijing 100029, China*
[4] *College of Earth Sciences, University of Chinese Academy of Sciences, Beijing 100049, China*
[5]*School of Atmospheric Physics, Nanjing University of Information Science and Technology, Nanjing 210044, China*
[6]*Earth System Science Interdisciplinary Center and Department of Atmospheric and Oceanic Science, University of Maryland, College Park, Maryland, USA*

Correspondence to: Fang.zhang@bnu.edu.cn

Abstract

The effects of aerosols on visibility through scattering and absorption of light and on climate through altering cloud droplet concentration are closely associated with their hygroscopic properties. Here, based on field campaigns in winter and summer in Beijing, we compare the size-resolved hygroscopic parameter (κ_{gf}) of ambient fine particles derived by an HTDMA (Hygroscopic Tandem Differential Mobility Analyzer) to that (denoted as κ_{chem}) of calculated by an HR-ToF-AMS (High-resolution Time-of-Flight Aerosol Mass Spectrometer) measurements using a simple rule with a uniform internal mixing hypothesis. We mainly focus on contrasting the disparity of κ_{gf} and κ_{chem} between summer and winter to reveal the impact of atmospheric processes/sources on aerosols hygroscopicity and to evaluate the uncertainty in estimating particles hygroscopicity with the hypothesis. We show that, in summer, the κ_{chem} for 110, 150 and 200 nm particles was averagely ~10% - 12% lower than κ_{gf}, with the greatest difference between the values observed around noontime when aerosols experience rapid photochemical aging. In winter, no apparent disparity between κ_{chem} and κ_{gf} is observed for those >100 nm particles around noontime, but the κ_{chem} is much higher than κ_{gf} in the late afternoon when ambient aerosols are greatly influenced by local traffic and cooking

https://doi.org/10.5194/acp-2019-583
Preprint. Discussion started: 25 June 2019

Atmospheric Chemistry and Physics Discussions

sources. By comparing with the observation from other two sites (Xingtai, Hebei and Xinzhou, Shanxi) of north China, we verify that atmospheric photochemical aging of aerosols enhances their hygroscopicity and may induce a coating effect which thereby leads to 10%-20% underestimation of the hygroscopic parameter if using the uniform internal mixing assumption. The coating effect is found more significant for these >100 nm particles observed in remote or clean regions. However, local primary sources, which result in an externally mixture of the fine particles with a large number of POA (Primary Organic Aerosol) in urban Beijing, makes the particle much less hygroscopic and cause 20-40% overestimation of the hygroscopic parameter by the mixing rule assumption. In addition, we also note lower κ_{chem} than κ_{gf} for 80, 110 and 150 nm particles during the nighttime of winter, particularly in polluted days, probably due to a nighttime coating effect driven by condensation of secondary hygroscopic species on pre-existing aerosols in cold season. Our results suggest that it is critical to parameterize the impacts in model simulations to improve the evaluation of the aerosols indirect effect.

1. Introduction

The effects of aerosols on visibility through scattering and absorption of light and on climate through altering cloud droplet concentration are influenced by their hygroscopic growth. Understanding and reducing the uncertainty in prediction of the aerosol hygroscopic parameter (κ) using chemical composition would improve model predictions of aerosol effects on clouds and climate.

The hygroscopic parameter, κ, is dependent upon particle chemical composition (Gunthe et al., 2009). The hygroscopic properties of an aerosol, in addition to being affected by its chemical composition, are also affected by the particle mixing state. The mixing state of aerosol particles can be divided into external mixing and internal mixing. The chemical components in the aerosol particles are independent of each other. The chemical composition of the different types of aerosol particles is different within a certain particle size range, and the mixed state is external mixing. As the aerosol particles undergo transport, coagulation, and aging/coating in the atmosphere, the chemical components become more uniformly mixed within each particle size range, with the aerosol mixing state approaching an internal mixture. Depending on the physical properties of the different aerosol components, internal mixing can be divided into uniform internal mixing

https://doi.org/10.5194/acp-2019-583
Preprint. Discussion started: 25 June 2019


Atmospheric Chemistry and Physics Discussions

and "core-shell" mixing (Jacobson, 2001). For uniform internal mixing the distribution of the chemical components is the same throughout each particle. "Core-shell" mixing refers to a mixing state in which certain chemical components are coated or coagulated on the surface of other chemical components (such as black carbon) during aging. In the atmosphere, the aerosol sources and sinks are varied, the physical and chemical processes experienced by the aerosols are complex, and the mixing state is more complicated. In heavily polluted areas, BC is usually mixed with other chemical components. Freshly emitted BC is mostly in an external mixed state. With the aging process, it gradually transforms into the internal mixing state (Chen, et al., 2016; Lee, et al., 2015; Wang, et al., 2017). Based on observations in the winter of Beijing urban area, Wang et al. (2019) found that the secondary aerosol generated from photochemical reactions is thickly coated on the surface of BC.

Studies have shown that the difference between the κ obtained using H-TDMA data, κ_{gf}, and that calculated based on the volume mixing ratio of chemical components, κ_{chem}, depends on the mixing state and the extent of aging of the particles (Mikhailov, et al., 2015; Zhang et al., 2017). Results from Cruz and Pandis (2000) also indicate that κ_{gf} of internally mixed ammonium sulfate and organic matter is higher than κ_{chem} calculated for assumed uniform internal mixing. Similarly, in some studies on aged aerosols (Bougiatioti, et al., 2009; Chang, et al., 2007; Kuwata, et al., 2008; Wang, et al., 2010), the concentration of CCN was underestimated by the calculation based on uniform internal mixing. Our previous study demonstrated that particle mixing state has large impacts on prediction of CCN concentration for the aerosol sampled in Beijing (Ren et al., 2018). Zhang et al. (2017) observed an evident underestimation of around noontime particle hygroscopicity based on chemical composition measurements in urban Beijing. Wang et al. (2018a) also noted a lower hygroscopic parameter estimated by the simple volume mixing ratio than that derived from direct HTDMA measurement at a site in North China Plain. These studies have revealed the uncertainty in the estimation of aerosol hygroscopicity parameters using chemical composition volume mixing ratios with the assumption that of uniform internal mixing, but there is still lack of a systematic investigation on the cause and magnitude of the effect. Furthermore, most studies that have been conducted compare the size-resolved hygroscopic parameter κ obtained with an HTDMA with κ calculated from bulk

https://doi.org/10.5194/acp-2019-583
Preprint. Discussion started: 25 June 2019

chemical composition measurements, motivating our analysis that employs size-resolved chemical composition measured by an HR-ToF-AMS.

The aim of this paper is to study the hygroscopicity and mixing state characteristics of fine particles in the Beijing urban area, and to reveal the impact of atmospheric processes/sources on aerosols hygroscopicity and elucidate the uncertainty in calculating the hygroscopic parameter using simple mixing rule estimates based on size-resolved chemical composition. The experiment and theory in the study are introduced in Sect. 2. The comparison between the hygroscopic parameter obtained from the HTDMA and and that calculated using size-resolved chemical composition is discussed in Sect. 3. Conclusions from the study are given in Sect. 4.

2. Experiment and Theory

2.1. Site and instruments

In this study, we mainly focus on analysis of the data obtained from two campaigns in urban Beijing (BJ: 39.97 ° N, 116.37 ° E). In addition, we also compare the results from the field campaigns with those from two sites, Xingtai (XT: 37.18 °N，114.37 °E), and Xinzhou (XZ: 38.24 °N，112.43 °E), in North China Plain (Fig. 1). The BJ site is located at the Institute of Atmospheric Physics (IAP), Chinese Academy of Sciences, which is between the north third and fourth ring roads in northern Beijing. Local traffic and cooking emissions can be important at the site (Sun et al., 2015). The sampling period in cold season was from 16 November to 10 December 2016, during the domestic heating period in Beijing. The sampling period in warm season was from 25 May to 18 June 2017. The XT site is located in the National Meteorological Basic Station, which is about 17 km from the XT urban area. The sampling period was from 17 May to 14 June 2016. Xingtai, with a high level of industrialization and urbanization, is located in the center of the North China Plain. Due to industrial emissions and typically weak ventilating winds, concentrations of $PM_{2.5,}$ black carbon and gaseous precursors are extremely high at the Xingtai site (Fu et al., 2014). Xinzhou is located north of Taiyuan and about 360 km southwest of Beijing, in the north central part of Shanxi Province, and is surrounded by mountains on three sides. The XZ site is located in a town,

https://doi.org/10.5194/acp-2019-583
Preprint. Discussion started: 25 June 2019

Atmospheric Chemistry and Physics Discussions

surrounded by agricultural land (such as corn fields). Local emissions from motor vehicles and industrial activities have relatively little influence on the sampled aerosol (Zhang et al., 2016). Because of its location and elevation, the aerosol at the XZ site is usually aged and transported from other areas. The sampling period was from July 22 to August 26, 2014 at XZ site.

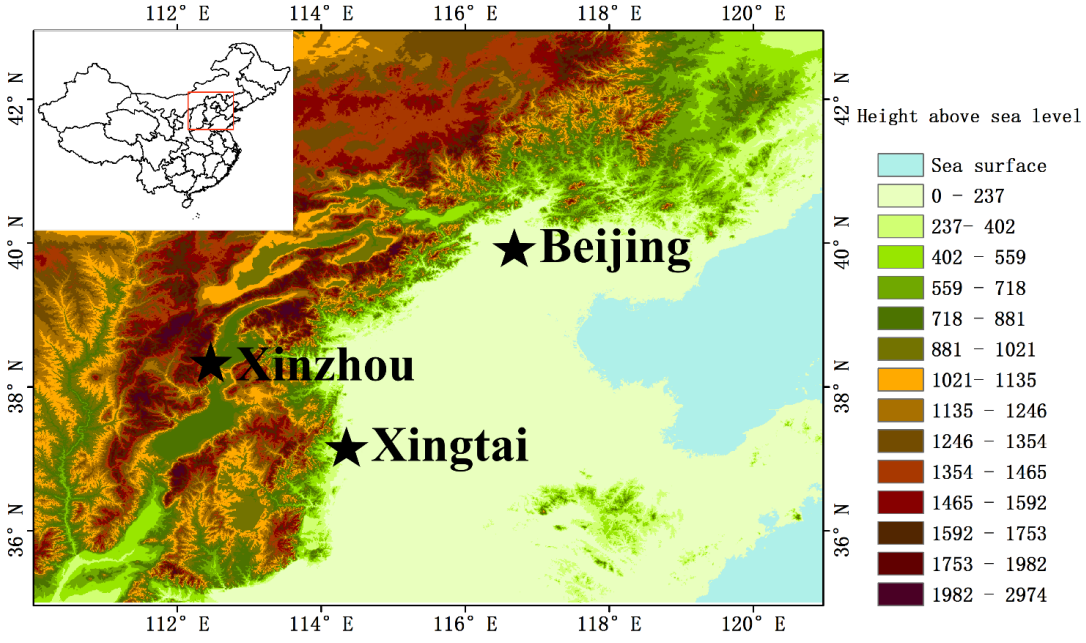

Figure 1. The map location of the sites

Particle number size distribution (PNSD) in the size range from 10 nm to 550 nm was measured with a Scanning Mobility Particle Sizer (SMPS; Wang & Flagan, 1990; Collins et al., 2002), which consists of a long differential mobility analyzer (DMA, model 3081L, TSI Inc) to classify the particle and a condensation particle counter (CPC, model 3772, TSI Inc.) to detect the size classified particles. The sampled particles were dried to relative humidity < 30% before entering the DMA. The measurement time for each size distribution was five minutes.

The HTDMA system used in this study has been described in detail in previous publications (Tan et al., 2013; Wang et al., 2017; Zhang et al., 2017). Here, only a brief description is given. A Nafion dryer dried

https://doi.org/10.5194/acp-2019-583
Preprint. Discussion started: 25 June 2019


Atmospheric Chemistry and Physics Discussions

125 the sampled particles to relative humidity < 20%, after which the steady state charge distribution was
126 reached in a bipolar neutralizer. The first differential mobility analyzer (DMA_1, model 3081L, TSI Inc.)
127 selected the quasi-monodisperse particles through applying a fixed voltage. The dry diameters selected in
128 this study were 40, 80, 110, 150, and 200 nm. The quasi-monodisperse particles were humidified to a
129 controlled RH (90% in this study) using a Nafion humidifier. A second DMA (DMA_2, same model as the
130 DMA_1) coupled with a water-based condensation particle counter (WCPC, model 3787, TSI Inc.) measured
131 the particle number size distributions of the humidified aerosol. RH calibration with ammonium sulfate was
132 carried out regularly during the study.

133 The hygroscopic growth factor (Gf) is defined as the ratio of the mobility diameter at a given RH to the
134 dry diameter:

$$\mathrm{Gf} = \frac{D(RH)}{D(dry)}$$

135 The Gf probability density function is retrieved based on the $TDMA_{inv}$ algorithm developed by Gysel et
136 al. (2009). Dry scans in which the RH between the two DMAs was not increased were used to define the
137 width of the transfer function.

138 Size-resolved non-refractory submicron aerosol composition was measured with an Aerodyne
139 high-resolution time-of-flight aerosol mass spectrometer (HR-ToF-AMS; Xu et al., 2015). The particle
140 mobility diameter was estimated by dividing the vacuum aerodynamic diameter from the AMS
141 measurements by particle density. Because the uncertainty caused by the fixed density across the size range
142 is negligible (Wang et al. 2016), here, the particle density is assumed to be 1600 kg m^{-3} (Hu et al., 2012).
143 AMS positive matrix factorization (PMF) with the PMF2.exe (v4.2) method was performed to identify
144 various factors of organic aerosols. Xu et al. (2015) have described the operation and calibration of the
145 HR-ToF-AMS in detail. Black carbon (BC) mass concentration was derived from measurements of light
146 absorption with a 7-wavelength aethalometer (AE33, Magee Scientific Corp.; Zhao et al., 2017).

https://doi.org/10.5194/acp-2019-583
Preprint. Discussion started: 25 June 2019


Atmospheric Chemistry and Physics Discussions

147 **2.2. Data**

148 The time series of the submicron particle mass concentration PM_1, (Fig. 2a), bulk mass concentrations
149 of the main species in PM_1 (Fig. 2b), mass fraction of the chemical composition of PM_1 (Fig. 2c), and
150 Gf-PDFs for 40, 80, 110, 150, 200 nm particles (Fig. 2d-h) during the campaign are presented in Fig. 2. As
151 shown in Fig. 2, quite distinct temporal variability of aerosol chemical and physical properties was observed
152 between winter and summer. The average mass concentration of PM_1 was 55.2 $\mu g/m^3$ in the winter and 16.5
153 $\mu g/m^3$ in the summer during our study periods. In this study, we define the conditions when the mass
154 concentration in winter period was < 20 $\mu g\ m^{-3}$ and >80 $\mu g\ m^{-3}$ as clean and polluted conditions, respectively.
155 Organic aerosol (OA), consisting of secondary organic aerosol (SOA) and primary organic aerosol (POA),
156 was the major fraction during both the winter and summer sampling periods. POA concentration was higher
157 than that of SOA in the winter, which reflects the influence of primary emissions such as coal combustion
158 OA (COOA) in Beijing (Hu et al., 2016; Sun et al., 2016). In contrast, SOA usually dominated in the
159 summer, which is evidence that secondary aerosol formation played a key role in the source of PM_1. Figs.
160 2d-h show the time series of the probability density functions (PDFs) of GF for 40, 80, 110, 150, and 200
161 nm particles, respectively. Distinct hydrophobic (with Gf of ~1.0) and more hygroscopic (with Gf of ~1.5)
162 modes were observed from Gf-PDFs of both small and large particles. Sometimes the more hygroscopic
163 mode particles were more concentrated and at others the hydrophobic particles were. In general though, the
164 more hygroscopic mode dominated for larger particles (i.e. 150 and 200 nm), and the less hygroscopic mode
165 did for the smallest particles (e.g. 40 nm) (Fig. 2d-h and Fig. S1). Occasionally, only the hydrophobic mode
166 was evident for 150 and 200 nm particles, which occurred when POA dominated the PM_1. Only the
167 hygroscopic mode was discernable for 40 nm particles during new particle formation (NPF) events that
168 occurred more frequently in summer than winter (Fig. S2).

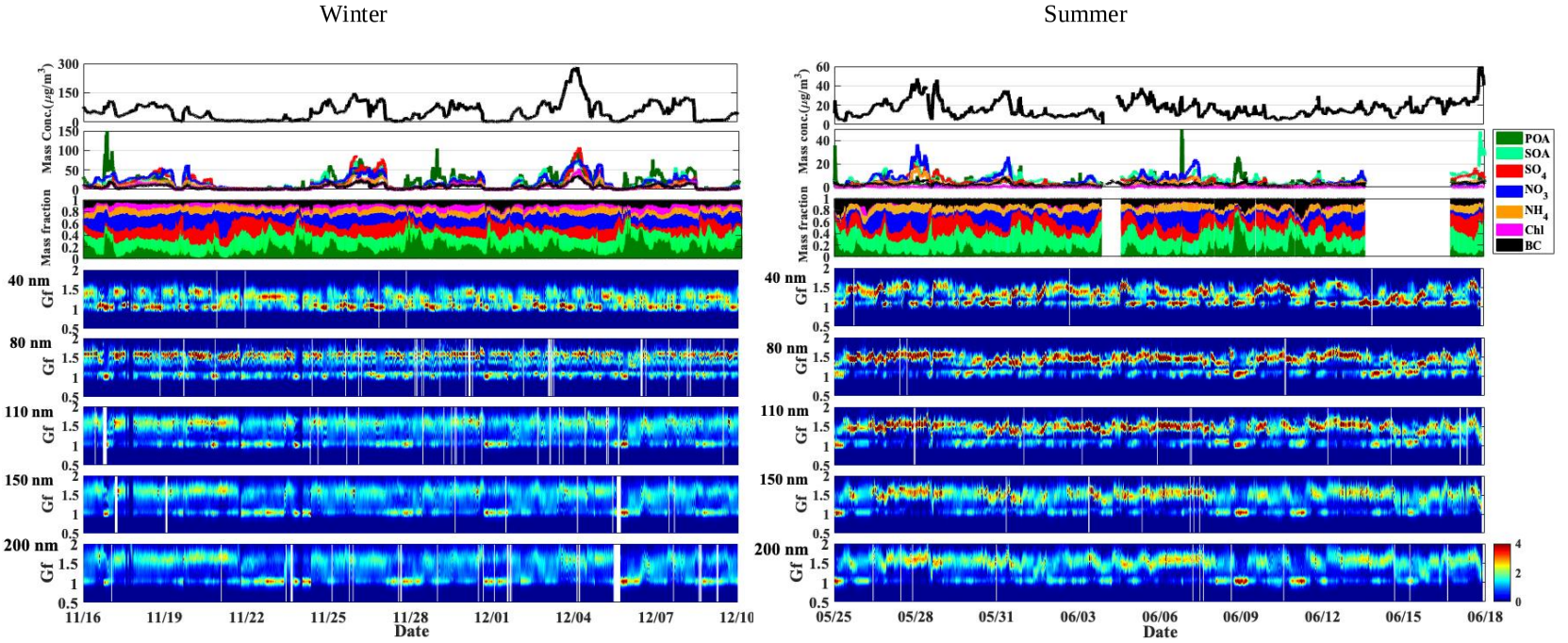

Figure 2. Winter (left) and summer (right) time series of (a) mass concentration of PM1; (b) bulk mass concentration of the main species in PM1; (c) mass fraction of the chemical composition of PM1; (d-h) Gf-PDFs for 40, 80, 110, 150 and 200 nm particles.

https://doi.org/10.5194/acp-2019-583
Preprint. Discussion started: 25 June 2019

Atmospheric Chemistry and Physics Discussions

2.3. Theory and method

2.3.1 Derivation of the hygroscopic parameter, κ, from the growth factor (Gf)

According to κ -Köhler Theory (Petters and Kreidenweis, 2007), the hygroscopicity parameter κ can be derived using the growth factor measured by an HTDMA.

$$\kappa = (Gf^3 - 1)\left(\frac{\exp\left(\frac{A}{D_d Gf}\right)}{RH} - 1\right) \quad , \tag{1}$$

$$A = \frac{4\sigma_{s/a} M_w}{RT\rho_w} \quad , \tag{2}$$

where Gf is hygroscopic growth factor measured by HTDMA, D_d is the dry diameter of the particles, RH is the relative humidity in the HTDMA (90%, in our study), $\sigma_{S/a}$ is the surface tension of the solution/air (assumed here to be the surface tension of pure water, $\sigma_{S/a}$ = 0.0728 N m^{-2}), M_w is the molecular weight of water, R is the universal gas constant, T is the absolute temperature, and ρ_w is the density of water.

2.3.2 Derivation of the hygroscopic parameter, κ, from chemical composition data

For an assumed internal mixture, κ can also be calculated by a simple mixing rule on the basis of chemical volume fractions (Petters and Kreidenweis, 2007; Gunthe et al., 2009):

$$\kappa_{chem} = \sum_i \varepsilon_i \kappa_i \quad , \tag{3}$$

$$\kappa_{org} = f_{POA} * \kappa_{POA} + f_{SOA} * \kappa_{SOA} \, , \tag{4}$$

where κ_i and ε_i are the hygroscopicity parameter and volume fraction for the ith individual (dry) component in the mixture, respectively, and f_{POA} and f_{SOA} are the volume fractions of POA and SOA in the organic component. The AMS provides mass concentrations of organics and of many inorganic ions. The inorganic components mainly consisted of $(NH_4)_2SO_4$ and NH_4NO_3 (Zhang et al., 2014; Zhang, et al., 2016; Zhang et al., 2017). As noted above, the organic components mainly consisted of POA and SOA. According to

https://doi.org/10.5194/acp-2019-583
Preprint. Discussion started: 25 June 2019

Atmospheric Chemistry and Physics Discussions

previous study, the values of κ are 0.48 for $(NH_4)_2SO_4$ and 0.58 for NH_4NO_3 (Petters and Kreidenweis, 2007). To estimate κ_{org} we used the following linear function derived by Mei et al. (2013): $\kappa_{org} = 2.10 \times f_{44} - 0.11$. We derived the volume fraction of each species by dividing mass concentration by its density. The values of density are 1720 kg m^{-3} for $(NH_4)_2SO_4$ and 1770 kg m^{-3} for NH_4NO_3. The densities of all organics, POA, and SOA are assumed to be 1200 kg m^{-3} (Turpin et al., 2001), 1000 kg m^{-3} , and 1400 kg m^{-3} respectively. The κ and density ofBC are assumed to be 0 and 1700 kg m^{-3}. In the following discussions, κ_{gf} and κ_{chem} denote the values derived from HTDMA measurements and calculated using the ZSR mixing rule, respectively.

3. Results and discussion

3.1. Diurnal variations of ambient fine particles physiochemical properties and hygroscopic growth factor

The diurnal variations of the PNSD, mass concentration of PM_1, mass concentration and fraction of chemical components in PM_1, and Gf-PDFs for 40 and 150 nm particles during the campaign are shown in Fig. 3. During the summer an obvious peak value in the PNSD is observed around noontime due to NPF events that typically started around 10:00 LT (Local Time). The resulting sharp increase in number concentration of nucleation mode particles was followed by decreased concentration and a rapid growth in diameter of the particles along with increased mass concentration of SOA and sulfate in PM_1, indicating strong photochemical and secondary formation processes during daytime in the summer. In contrast, NPF was not evident during the winter period, which may in part be due to the much higher (~3x) PM_1 mass concentrations in the winter than in the summer. Note that peak values in number concentration and in mass concentrations of PM_1 and POA occurred during the early evening (17:00-21:00, LT) indicating the strong impact of local sources from traffic emissions and cooking. In addition, the diurnal cycles of aerosol physical and chemical properties are also influenced by the diurnal changes in the planetary boundary layer (PBL) that leads to accumulation of particles during nighttime when higher values of both number and mass concentration were observed.

https://doi.org/10.5194/acp-2019-583
Preprint. Discussion started: 25 June 2019

Atmospheric Chemistry and Physics Discussions

Fig. 3e shows the diurnal variations of the Gf-PDFs for 40 nm and 150 nm particles. Owing to the continued local and primary emissions near the study site, the Gf-PDFs for 40 nm particles generally display a bimodal shape with more and less hygroscopic modes (with Gf of ~ 1.5 and ~ 1.1 respectively) throughout the day both in winter and summer periods, indicating an external mixing state for the 40 nm particles. Note that, during nighttime and early morning in the winter, the more hygroscopic mode dominated and was shifted to higher Gf than during the daytime. This is thought to be due to heterogeneous/aqueous reactions on pre-existing primary small particles, and/or coagulation/condensation processes that are enhanced at night under lower ambient temperature and higher relative humidity, all of which result in a more hygroscopic and more internally-mixed aerosol (Liu et al., 2011; Massling et al., 2005; Ye et al., 2013; Wu et al., 2016; Wang et al., 2018a).). Interestingly, in the summer period, the concentration of the hydrophilic mode increased quickly around noontime and in the early afternoon (12:00-16:00), with a corresponding decrease in the relative concentration of the hydrophobic mode, which likely indicates a transformation of the particles from externally to internally mixing state as a result of the species condensation from the photochemical reaction (Wu et al., 2016; Wang et al., 2017), resulting in an increase in particle hygroscopicity (Fig. S3). For 150 nm particles, the hygroscopic mode in the Gf-PDF is more dominant during daytime in particular during the summer period when the strong solar radiation promotes photochemical aging and growth, thus producing a more internally-mixed aerosol. The dominant hydrophobic mode at around 18:00 was observed both in winter and summer and reflects abundant traffic emissions and cooking sources (primarily with POA) during the early evening period (Fig. 2c).

https://doi.org/10.5194/acp-2019-583
Preprint. Discussion started: 25 June 2019

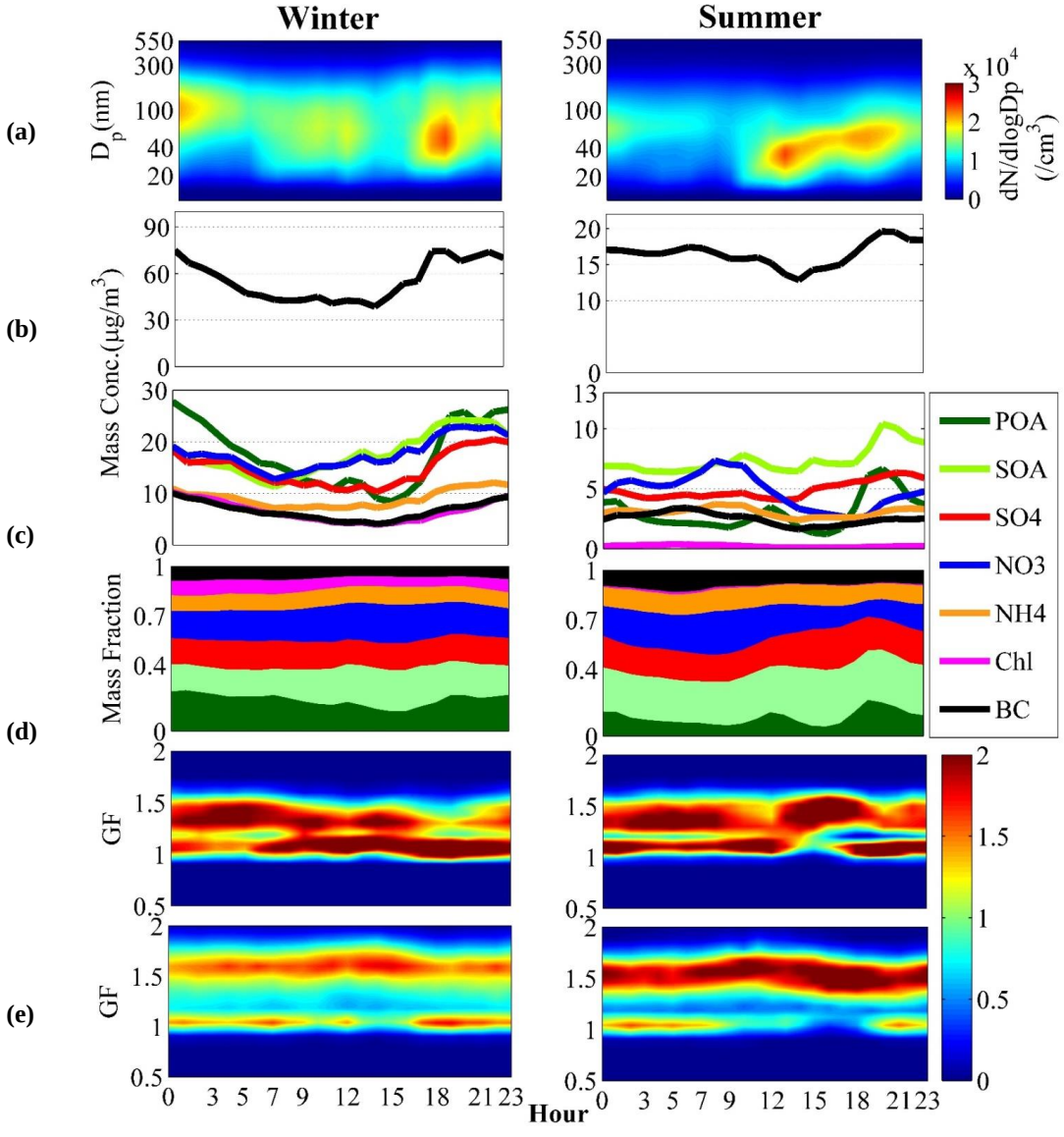

Figure 3. Diurnal variations in (a) particle number size distribution; (b) mass concentration of PM_1; (c) bulk mass concentration of main species in PM_1; (d) mass fraction of chemical composition of PM_1; (e) Gf-PDFs for 40 and 150 nm particles in winter and summer period respectively.

3.2 κ_{gf} dependence on D_p

The size dependence of particle hygroscopicity parameters for the winter and summer periods are presented in Fig.4. In the winter, the 40 nm particles were least hygroscopic and the hygroscopicity of larger

https://doi.org/10.5194/acp-2019-583
Preprint. Discussion started: 25 June 2019

Atmospheric Chemistry and Physics Discussions

particles (>80 nm) displayed insignificant dependence on particle size. The size independence for the larger particles is consistent with the observed similarity in mass fractions of inorganic and organic species across

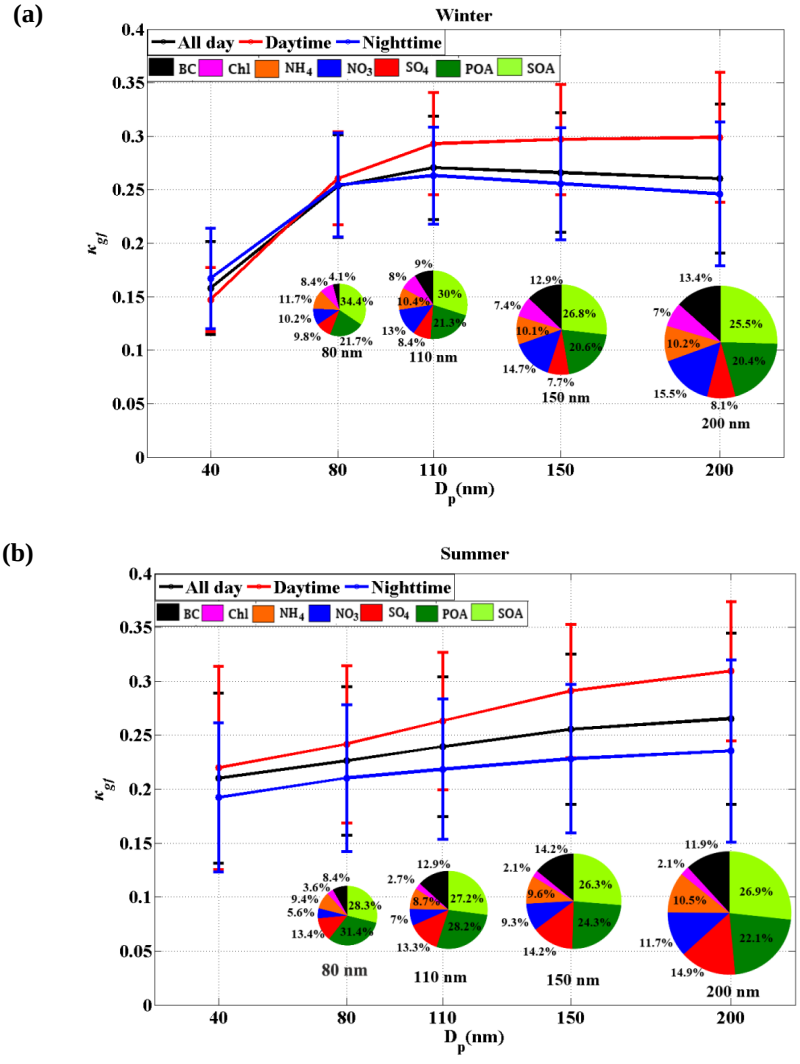

Figure 4. The dependence of κ on D_p at the urban Beijing site during the study periods. The κ values are retrieved from the size-resolved HTDMA measurements. The error bars represent $\pm 1\sigma$. The size-resolved chemical mass fractions at the corresponding D_p is also presented.

the size range as shown in the pie charts in Figure 4a. A similar dependence of particle hygroscopicity on particle size was also observed in the urban area of Beijing during the wintertime of 2014 (Wang et al., 2018b). In the summer, hygroscopicity increased with increasing particle size, which is expected based on

https://doi.org/10.5194/acp-2019-583
Preprint. Discussion started: 25 June 2019

Atmospheric Chemistry and Physics Discussions

the size dependent patterns shown in the pie charts, with the mass fraction of POA decreasing with the particles size and the mass fraction of inorganics like sulfate and nitrate increasing with particle size.

3.3. Closure of HTDMA and chemical composition derived κ

A closure study was conducted between κ_{chem} and κ_{gf} (Fig. 5) to investigate the uncertainty of the two methods, and especially to further illustrate whether particle hygroscopicity can be well predicted by κ_{chem} calculated by assuming internal mixing. Since a size-resolved BC mass concentration measurement was not available during the campaign, we use the bulk mass fraction of BC particles measured by the AE33 combining with size-resolved BC distribution in Beijing reported by Liu et al. (2018) to estimate κ_{chem}.

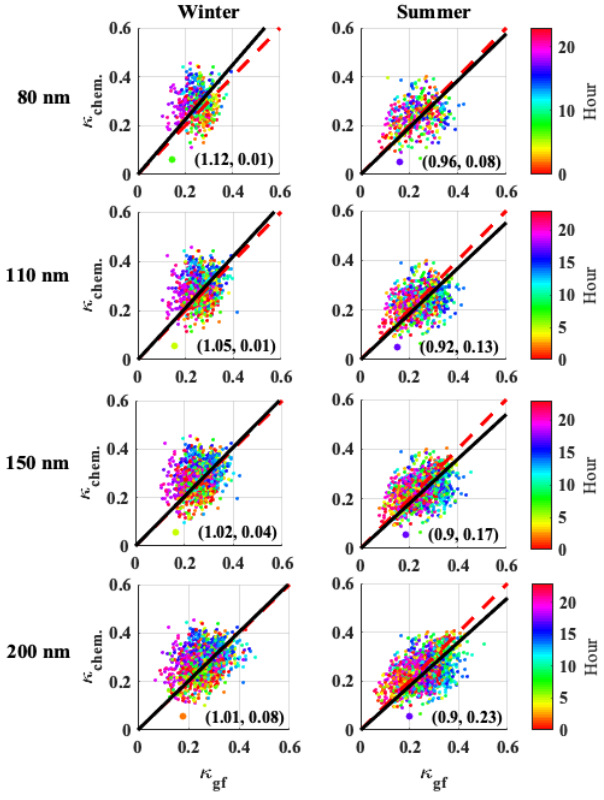

Figure 5. Closure of κ_{chem} calculated from size-resolved chemical composition data and κ_{gf} retrieved from hygroscopic growth factor by HTDMA measurements in winter (left panels) and summer (right panels) period. The dots with different color correspond to observed time of a day during the campaign as shown by the color bar. The number in parentheses is correlation coefficients (R^2) and slopes of linear fits.

https://doi.org/10.5194/acp-2019-583
Preprint. Discussion started: 25 June 2019

Atmospheric Chemistry and Physics Discussions

Uncertainty in κ is due in part to measurement uncertainty of the HTDMA/CCNc system and uncertainty resulting from non-ideality effects in the solution droplets, surface tension reduction due to surface active substances, and the presence of slightly soluble substances that dissolve at RH higher than that maintained in the HTDMA (e.g., Wex et al., 2009; Good et al., 2010; Irwin et al., 2010; Cerully et al., 2011; Wu et al., 2013). However, our previous study demonstrated that, for this region, estimates using HTDMA data are still better than those using the simple mixing rule based on chemical volume fractions for an assumed internal mixture (Zhang et al., 2017). Therefore, here we focus on discussing and exploring the uncertainty of κ_{chem} by taking κ_{gf} as the reference.

Our results show that, in winter, the slopes from linear fitting of κ_{chem} and κ_{gf} are about 0.96-1.0 for particles with diameters of 80, 110, 150, and 200 nm, indicating an overall consistency of κ_{chem} and κ_{gf}. In summer, the slopes are 0.88-0.89 for 110, 150, and 200 nm particles, meaning there is about 10% - 12% underestimation of κ_{chem}. However, the poor correlations (typically with correlation coefficients, R^2, of < 0.3) between κ_{chem} and κ_{gf} of the 80, 110, 150, 200 nm particles both in winter and summer reflect large uncertainty in one or both of the calculated parameters. The large uncertainties are likely due to the unreasonable assumption of particle mixing state (e.g. Cruz and Pandis, 2000; Svenningsson et al., 2006; Sjogren et al., 2007; Zardini et al., 2008), which varies with their aging and other physiochemical processes in the atmosphere. For example, underestimation of κ_{chem} for the summer occurred mostly in the afternoon. This may be associated with photochemical processes at around noontime. More specific investigations of the particle mixing and aging impacts on κ_{chem} will be further addressed in the following sections.

3.4 Atmospheric processes and sources effects indicated by diurnal cycles of κ_{chem} and κ_{gf}

The diurnal cycles of particle hygroscopicity in the summer and winter with the use of the size-resolved chemical composition observations and the ratio of κ_{chem} to κ_{gf} are shown in Fig. 6. In summer, at 09:00-15:00, the disparity between κ_{chem} and κ_{gf} is insignificant for smaller particles (80 and 110 nm), both of which show slight decrease from 09:00 or 10:00 to 12:00-13:00 due to the frequent NPF event that usually corresponds to a large fraction of organics (Fig. 3) in urban Beijing. For larger particles (150 and 200 nm), the disparity between κ_{chem} and κ_{gf} around noontime and in the early afternoon is very significant,

https://doi.org/10.5194/acp-2019-583
Preprint. Discussion started: 25 June 2019


Atmospheric Chemistry and Physics Discussions

293 corresponding to >20% underestimation of particle hygroscopisity by κ_{chem} (with the ratio of κ_{chem} to κ_{gf} of
294 ~0.8). Similar patterns were also noted by Zhang et al., (2017) but which is only based on a comparison
295 between κ_{chem} derived from bulk chemical composition and κ_{gf}. Our results further clarify that the rapid
296 photochemical aging of BC particles, which are generally with dominant size modes of 100-200 nm in the
297 atmosphere, leads to the core-shell structure in which certain secondary aerosol generated from
298 photochemical reactions is thickly coated on the surface of BC (Wang et al., 2019). The hygroscopicity of
299 the coated BC particles may only depend on the coating layer (Ma et al., 2013), thus resulting in the
300 noontime/early afternoon underestimation of particle hygroscopicity by κ_{chem}. While, no significant
301 differences between κ_{chem} and κ_{gf} are observed during night time. Note that κ_{chem} is slightly higher than κ_{gf}
302 during early evening traffic rush hour and cooking time, when emissions of primary hydrophobic particles
303 (e.g. POA) are high (Fig. 3b), thus resulting in a large percentage of externally-mixed particles (Fig. 3e, Fig.
304 S4 and Fig. S5). Therefore, the assumption of uniform internal mixing will overestimate hygroscopicity
305 according to our previous study (Zhang et al., 2017). But the particles experience rapid conversion and
306 mixing in urban Beijing due to high precursor gases (Sun et al., 2015; Wu et al., 2016; Ren et al., 2018), and
307 thus the coated/aged particles produced through photochemical processing in the afternoon can mix and
308 interact with and freshly emitted primary particles emitted during rush hour (Wu et al., 2008). Therefore,
309 during nighttime (22:00-06:00, LT), the particles are more uniform internally-mixed, which is reflective of
310 the assumption for calculation of κ_{chem}, a much better consistency between κ_{chem} and κ_{gf} is observed. And due
311 to the relatively clean conditions overall in the summer, no large differences are observed under clean and
312 polluted conditions (Fig. S5-S7).

https://doi.org/10.5194/acp-2019-583
Preprint. Discussion started: 25 June 2019

Atmospheric Chemistry and Physics Discussions

313

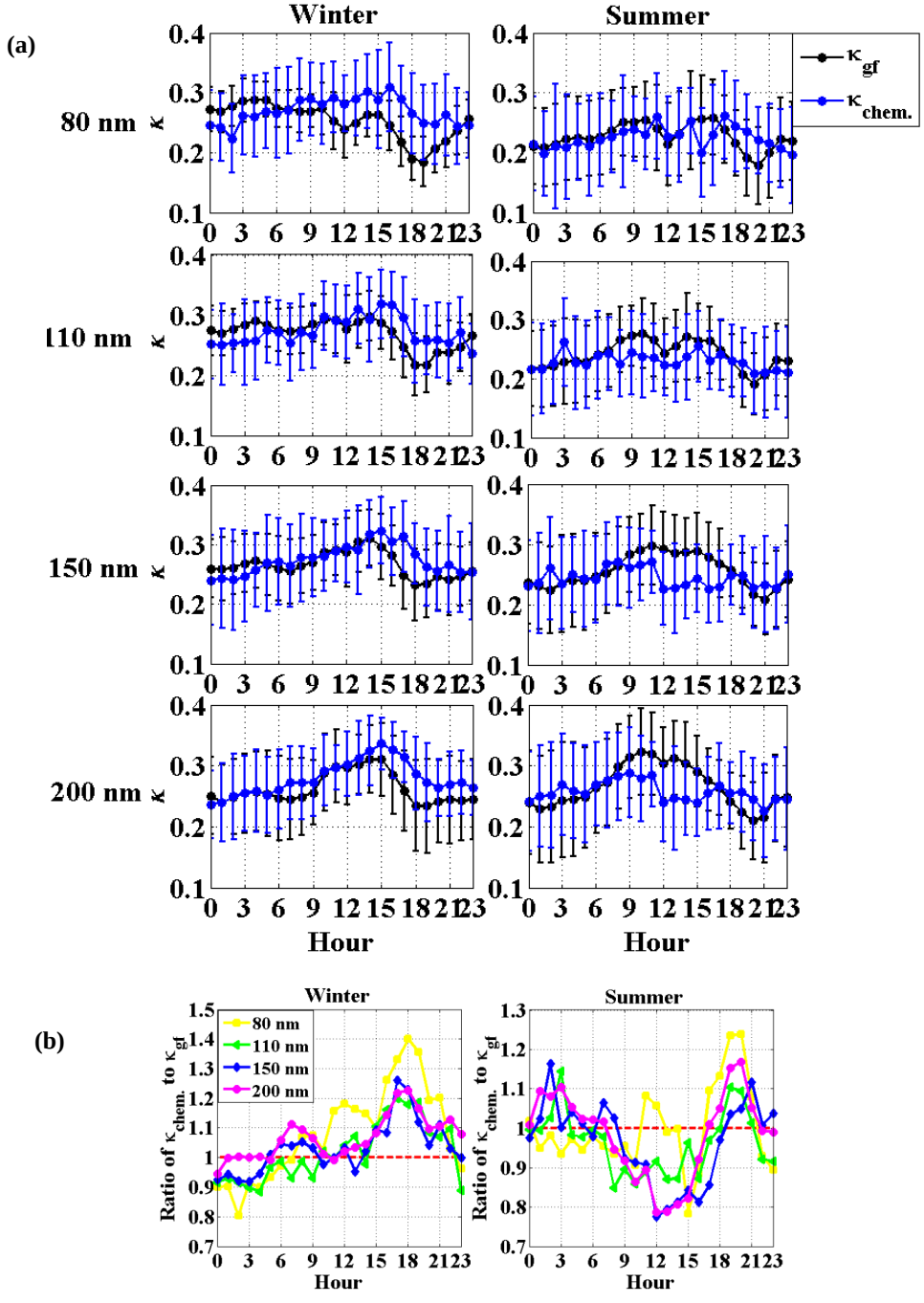

314

315

316 Figure 6. Diurnal variations in (a) κ_{chem} using size-resolved chemical composition data and κ_{gf} in winter and

317 summer period; and (b) ratio of κ_{chem} to κ_{gf} in winter and summer period.

https://doi.org/10.5194/acp-2019-583
Preprint. Discussion started: 25 June 2019

Atmospheric Chemistry and Physics Discussions

318 In winter, the disparity between κ_{chem} to κ_{gf} is insignificant at 09:00-15:00 due to the weakening
319 effect of photochemical aging. From 15:00 to 21:00 LT, due to the strong vehicle and cooking sources
320 around the site, the particles are dominated by the hydrophobic mode with a large concentration of
321 externally-mixed POA particles (Fig. 3 and Fig. S8), the calculated κ_{chem} is much higher than κ_{gf}, with the
322 maximum ratio of κ_{chem} to κ_{gf} of 1.2-1.4, and the greatest disparity is observed for small particles. The

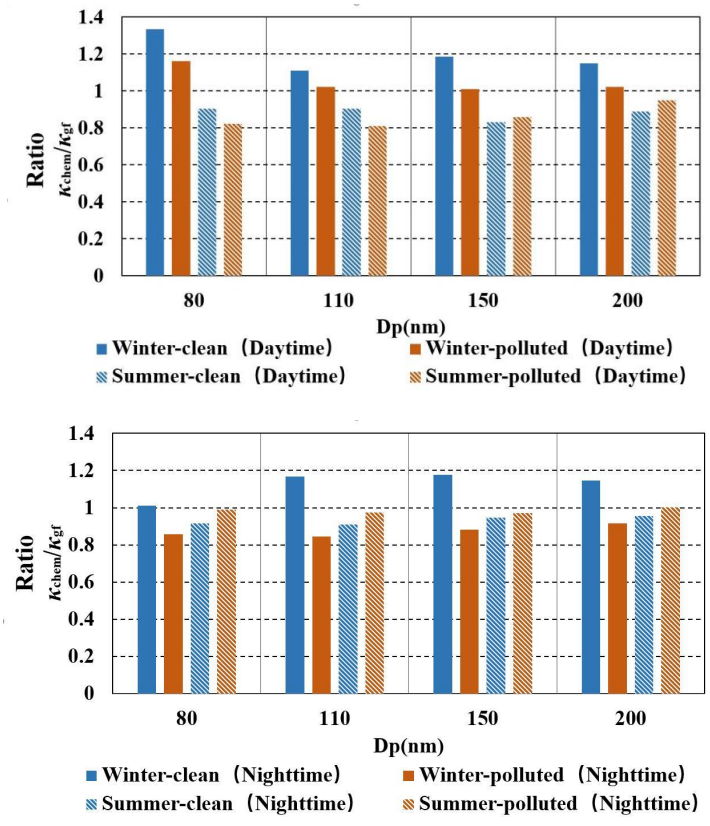

323
324

325 Figure 7. Ratio of mean κ_{chem} to κ_{gf} during daytime (top panel) and nighttime (bottom panel) under
326 clean /polluted conditions between winter and summer period.

327 disparity is further enhanced during clean periods (Fig. S7, Fig. S9 and Fig. 7) when the hydrophobic mode
328 is dominant (Fig. 8). But note that during the nighttime, κ_{chem} is slight lower than κ_{gf}, with the minimum ratio
329 of κ_{chem} to κ_{gf} of ~0.8 for 80 nm particles and ~0.9 for 110 and 150 nm particles at 02:00-04:00 LT (Fig. 6b),
330 indicating an underestimation of particle hygroscopicity using composition data. The disparity at nighttime
331 is further increased during heavily polluted events (Fig. 7 and Fig. S9), when the particles are more

https://doi.org/10.5194/acp-2019-583
Preprint. Discussion started: 25 June 2019

Atmospheric Chemistry and Physics Discussions

internally-mixed with only one hygroscopic mode (Fig. 8 and Fig. S8). We believe the increased underestimation during polluted conditions is likely due to enhanced condensation of secondary hygroscopic compounds (e.g. nitrate, sulfate) on pre-existing aerosols at lower temperature and higher relative humidity at nighttime (Wu et al., 2008; Wang et al., 2016; An et al., 2019).

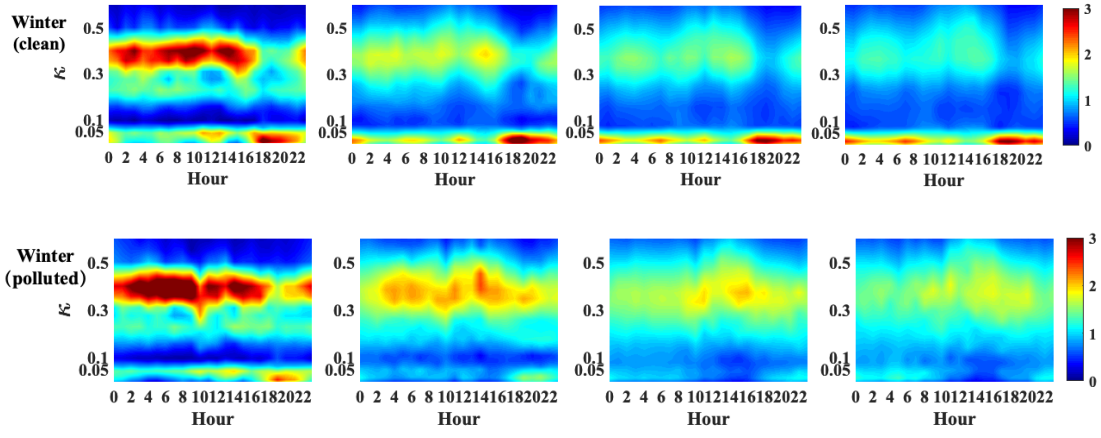

Figure 8. Diurnal cycles of κ_{gf} -PDF for 80, 110, 150 and 200 nm particles in clean and polluted events in winter.

3.5. Observation from other stations

The aging process in the summer period is related to photochemical processing in strong solar radiation conditions. The photochemical reactions produce sulfate and secondary organic aerosol, condensing on the surface of slightly- or non-hygroscopic primary aerosols (such as black carbon) (Zhang et al., 2008). As discussed in 3.4, the core-shell structure that accompanies aging of the particles results in calculated κ_{chem} that underestimates their hygroscopicity. To confirm such a coating effect on particle hygroscopicity, we further examine the diurnal variations of κ_{chem} and κ_{gf} or κ_{CCNc} (derived from CCN measurements) based on observations in summer at two other sites in north China (Fig. 1). We find that the case at the Xingtai (XT) site is very similar to that observed in Beijing (BJ), with a lower κ_{chem} than κ_{gf} around noon time. But, because of much less influences from the local sources at XT compared to that at BJ, such underestimation by κ_{chem} continued until night at XT (Fig. 9b). Interestingly, a noontime lower κ_{chem} was not observed in the diurnal cycles at the Xinzhou (XZ) site, where κ_{chem} and κ_{CCNc} had similar diurnal patterns (Fig. 9c) with a

https://doi.org/10.5194/acp-2019-583
Preprint. Discussion started: 25 June 2019

Atmospheric Chemistry and Physics Discussions

roughly constant ratio of κ_{chem} to κ_{CCNc} of ~0.8-0.9. This is probably because the XZ site is usually the recipient of aerosols transported from other areas that are already aged and well-mixed, with minimal impact of additional coating (Zhang et al., 2017). Also, the rate of oxidation and condensation may be slow in the relatively remote area where the gas precursors and oxidants are not as high as they are closer to sources regions. But at XT, which is located in the heavily polluted area in the north China Plain (Fu et al., 2014), aerosol emissions and processing are more similar to that in urban Beijing.

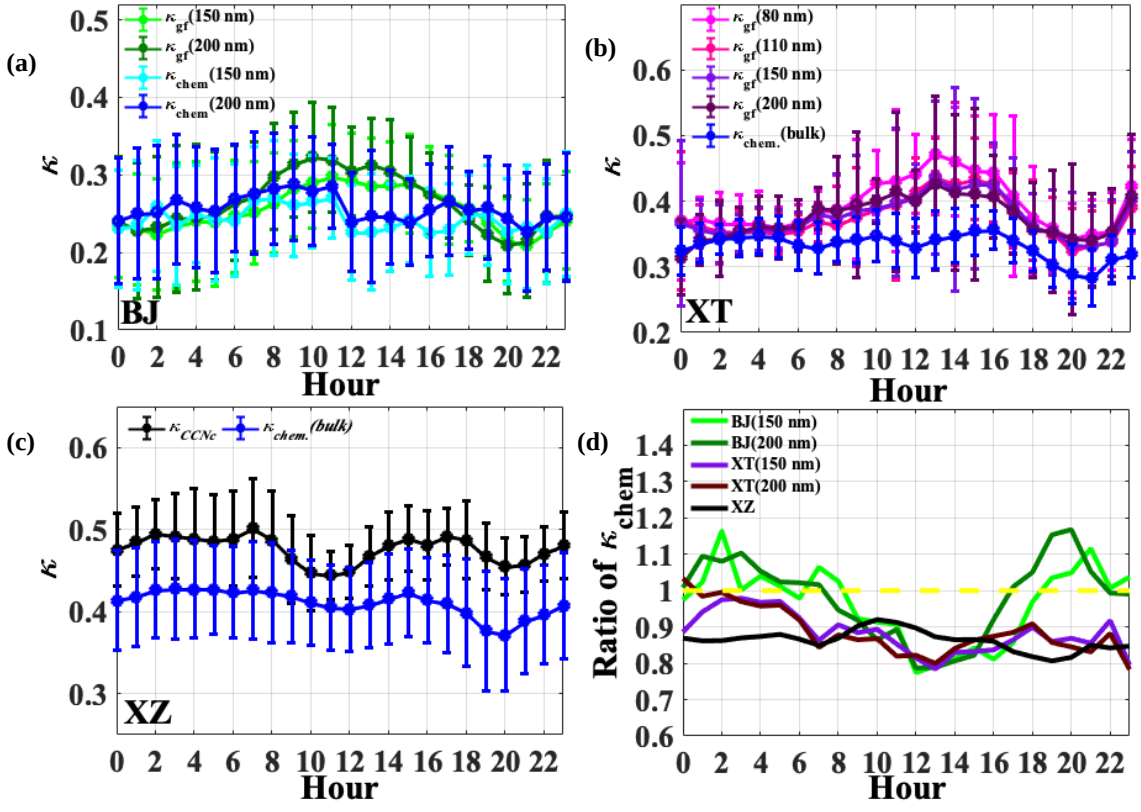

Figure 9. Diurnal variations in (a) κ_{chem} and κ_{gf} for 150 and 200 nm particles at BJ site; (b) κ_{chem} and κ_{gf} for 40, 80, 110, 150 and 200 nm particles at XT site; (c) κ_{chem} and mean κ_{CCNc} for particles at XZ site, and (d) ratio of mean κ_{chem} to κ_{gf} at the three sites.

Although the underestimation in κ_{chem} may be also related to the uncertainty in the hygroscopic parameter for organics, which is calculated from a simple parametrized equation based on the AMS-measured f_{44} value reported by Mei et al. (2013), Zhang et al. (2017) has shown that even the large

https://doi.org/10.5194/acp-2019-583
Preprint. Discussion started: 25 June 2019

underestimation of κ_{SOA} could not fully explain that of κ_{chem}. Furthermore, the value for f_{44} tends to be overestimated according to Fröhlich et al. (2015), which should lead to a larger κ_{chem}. Previous studies have shown that freshly emitted POA and BC particles may be rapidly coated by more hygroscopic components in polluted urban areas, resulting in enhanced hygroscopicity of the mixed particles (Zhang et al., 2004; Johnson et al., 2005; Zhao et al., 2017). Our results are consistent with those observations and clarify the photochemical aging and coating effect will largely underestimate the particles hygroscopisity using simple mixing rule based on chemical composition.

4. Conclusion

Using measurements of aerosol composition and hygroscopicity made in Beijing (BJ) during a winter period of 2016 and a summer period of 2017, this paper analyzes the daily variation and seasonal differences of size-resolved aerosol hygroscopicity in urban Beijing. We mainly focus on studying the disparity of κ_{gf} and κ_{chem} between summer and winter to reveal the impact of atmospheric processes and mixing state of the particles on its hygroscopicity. The uncertainty in calculating κ by using chemical composition with a uniform internal mixing hypothesis is elucidated from the diurnal variations of the difference between the calculated values: in summer, lower κ_{chem} is obtained around noontime, with a ratio of κ_{chem} to κ_{gf} of about 0.8-0.9 for large particles (i.e. 150 nm and 200 nm), showing an underestimation of particles hygroscopisity by using simple mixing rule based on chemical composition. Combining with the observation from Xingtai and Xinzhou, we attribute the underestimation to the rapid noontime photochemical aging processes in summer, which induces the coating effect that will lead to a lower κ if assuming a uniform mixing of the particles. In contrast, larger κ_{chem} than κ_{gf} for >100 nm particles around noontime and in the early afternoon is derived in winter, with the maximum ratio of κ_{chem} to κ_{gf} of 1.2-1.4 when the particles are dominated by the hydrophobic mode with a large number of externally-mixed POA particles from strong vehicle and cooking sources. We suggest that, by using the simple mixing rule, the particles hygroscopisity can be underestimated up to 10%-20% for aged aerosols due to the coating effect, but will be maximally overestimated 20-40% for externally-mixed particles. A lower κ_{chem} than κ_{gf} for 80, 110 and 150 nm particles during the nighttime of winter is also noted, and the disparity is further enlarged in polluted days, probably

https://doi.org/10.5194/acp-2019-583
Preprint. Discussion started: 25 June 2019


Atmospheric Chemistry and Physics Discussions

due to a nighttime coating effect driven by condensation of secondary hygroscopic species on pre-existing aerosols in cold season. Our results highlight the impacts of atmospheric processes, sources on aerosol mixing state and hygroscopicity, which should be quantified and considered in models for different atmospheric conditions. Long-term observations from more ground sites, as well as experiments in smog chambers, should be made to parameterize such impact in model simulations.

Data availability. All data needed to evaluate the conclusions in the paper are present in the paper and/or the Supplementary Materials. Also, all data used in the study are available from the corresponding author upon request (fang.zhang@bnu.edu.cn).

Author contributions. F.Z. and X.F. conceived the conceptual development of the manuscript. X. F. directed and performed of the experiments with L.C., X.J., Y. W., and F. Z.. X.F. and F.Z. conducted the data analysis and wrote the draft of the manuscript, and all authors edited and commented on the various sections of the manuscript.

Competing interests. The authors declare no competing interests.

Acknowledgements. This work was funded by the National Key R&D Program of China (grant no. 2017YFC1501702), National Natural Science Foundation of China (NSFC) research projects (grant nos. 41675141, 91544217). We thank all participants of the field campaign for their tireless work and cooperation.

References

An, Z., Huang, R. J., Zhang, R., Tie, X., Li, G., Cao, J., Zhou, W., Shi, Z., Han, Y., Gu, Z., & Ji, Y.: Severe haze in Northern China: A synergy of anthropogenic emissions and atmospheric processes, Proceedings of the National Academy of Sciences, 116(18), 8657-8666, doi:10.1073/pnas.1900125116, 2019.

Bougiatioti, A., Fountoukis, C., Kalivitis, N., Pandis, S. N., Nenes, A., & Mihalopoulos, N.: Cloud condensation nuclei measurements in the marine boundary layer of the Eastern Mediterranean: CCN closure and droplet growth kinetics, Atmos. Chem. Phys., 9, 7053–7066, doi: 10.5194/acp-9-7053-2009, 2009.

https://doi.org/10.5194/acp-2019-583
Preprint. Discussion started: 25 June 2019

417 Cerully, K. M., Raatikainen, T., Lance, S., Tkacik, D., Tiitta, P., Petäjä, T.,Nenes, A. : Aerosol
418 hygroscopicity and CCN activation kinetics in a boreal forest environment during the 2007 EUCAARI
419 campaign, Atmos. Chem. Phys., 11, 12369–12386, doi: 10.5194/acp-11-12369-2011, 2011.
420 Chang, R.-W., Liu, P., Leaitch, W., and Abbatt, J.: Comparison between measured and predicted CCN
421 concentrations at Egbert, Ontario: Focus on the organic aerosol fraction at a semi-rural site, Atmos.
422 Environ., 41, 8172–8182, 2007.
423 Chen, C., Fan, X., Shaltout, T., Qiu, C., Ma, Y., Goldman, A., and Khalizov, A. F.: An unexpected
424 restructuring of combustion soot aggregates by sub nanometer coatings of polycyclic aromatic
425 hydrocarbons, Geophys. Res. Lett., 43, 11080–11088, 2016.
426 Collins, D. R., Flagan, R. C., and Seinfeld, J. H.: Improved inversion of scanning DMA data, Aerosol Sci.
427 Technol., 36(1), 1–9, 2002.
428 Cruz, C. N. and Pandis, S. N.: Deliquescence and hygroscopic growth of mixed inorganic-organic
429 atmospheric aerosol, Environ. Sci. Technol., 34, 4313–4319, doi: 10.1021/es9907109, 2000.
430 DeCarlo, P. F., Kimmel, J. R., Trimborn, A., Northway, M. J., Jayne, J. T., Aiken, A. C., Gonin, M., Fuhrer,
431 K., Horvath, T., Docherty, K., Worsnop, D. R., and Jimenez, J. L.: Field-deployable, high-resolution,
432 time-of-flight aerosol mass spectrometer, Anal. Chem., 78, 8281–8289, doi: 10.1021/ac061249n, 2006.
433 Fors, E. O., Swietlicki, E., Svenningsson, B., Kristensson, A.,Frank, G. P., and Sporre, M.: Hygroscopic
434 properties of the ambient aerosol in southern Sweden – a two year study, Atmos. Chem. Phys., 11, 8343–
435 8361, doi: 10.5194/acp-11-8343-2011, 2011.
436 Fröhlich, R., Crenn, V., Setyan, A., Belis, C. A., Canonaco, F., Favez, O., Riffault, V., Slowik, J. G.,
437 Aas, W., Aijälä, M., Alastuey, A., Artiñano, B., Bonnaire, N., Bozzetti, C., Bressi, M.,Carbone, C., Coz,
438 E., Croteau, P. L., Cubison, M. J., Esser-Gietl,J. K., Green, D. C., Gros, V., Heikkinen, L., Herrmann, H.,
439 Jayne,J. T., Lunder, C. R., Minguillón, M. C., Mocnik, G., O'Dowd,C. D., Ovadnevaite, J., Petralia, E.,
440 Poulain, L., Priestman, M.,Ripoll, A., Sarda-Estève, R., Wiedensohler, A., Baltensperger,U., Sciare, J.,
441 and Prévôt, A. S. H.: ACTRIS ACSM intercomparison – Part 2: Intercomparison of ME-2 organic source
442 apportionment results from 15 individual, co-located aerosol mass spectrometers, Atmos. Meas. Tech., 8,
443 2555–2576, doi:10.5194/amt-8-2555-2015, 2015.

https://doi.org/10.5194/acp-2019-583
Preprint. Discussion started: 25 June 2019

444 Fu, G. Q., Xu, W. Y., Yang, R. F., Li, J. B., & Zhao, C. S. : The distribution and trends of fog and haze in
445 the North China Plain over the past 30 years, Atmos. Chem. Phys., 14, 11949-11958, doi:
446 10.5194/acp-14-11949-2014, 2014.
447 Gasparini, R., R. Li, and D. R. Collins: Integration of size distributions and size-resolved hygroscopicity
448 measured during the Houston Supersite for compositional categorization of the aerosol, Atmos. Environ.,
449 38, 3285–3303, doi:10.1016/j.atmosenv.2004.03.019, 2004.
450 Good, N., Topping, D. O., Allan, J. D., Flynn, M., Fuentes, E.,Irwin, M., Williams, P. I., Coe, H., and
451 McFiggans, G.: Consistency between parameterisations of aerosol hygroscopicity and CCN activity
452 during the RHaMBLe discovery cruise, Atmos. Chem. Phys., 10, 3189–3203, doi:
453 10.5194/acp-10-3189-2010, 2010.
454 Gunthe, S. S., King, S. M., Rose, D., Chen, Q., Roldin, P., Farmer,D. K., Jimenez, J. L., Artaxo, P., Andreae,
455 M. O., Martin, S.T., and Pöschl, U.: Cloud condensation nuclei in pristine tropical rainforest air of
456 Amazonia: size-resolved measurements and modeling of atmospheric aerosol composition and CCN
457 activity, Atmos. Chem. Phys., 9, 7551–7575, doi: 10.5194/acp-9-7551-2009, 2009.
458 Gysel, M., Crosier, J., Topping, D. O., Whitehead, J. D., Bower, K.N., Cubison, M. J., Williams, P. I., Flynn,
459 M. J., McFiggans, G.B., and Coe, H.: Closure study between chemical composition and hygroscopic
460 growth of aerosol particles during TORCH2, Atmos. Chem. Phys., 7, 6131–6144, doi:
461 10.5194/acp-7-6131-2007, 2007.
462 Gysel, M., McFiggans, G. B., and Coe, H.: Inversion of tandem differential mobility analyser (TDMA)
463 measurements, J. Aerosol Sci., 40, 134–151, doi: 10.1016/j.jaerosci.2008.07.013, 2009.
464 Hu, W., Hu, M., Hu, W., Jimenez, J. L., Yuan, B., Chen, W., Wang, M., Wu, Y., Chen, C., Wang, Z., Peng,
465 J., Zeng, L., and Shao, M.: Chemical composition, sources, and aging process of submicron aerosols in
466 Beijing: Contrast between summer and winter, J. Geophys. Res., 121, 1955–1977, doi:
467 10.1002/2015JD024020, 2016.
468 Irwin, M., Good, N., Crosier, J., Choularton, T. W., & McFiggans, G.: Reconciliation of measurements of
469 hygroscopic growth and critical supersaturation of aerosol particles in central Germany Atmos. Chem.
470 Phys., 10, 11737–11752, doi:10.5194/acp-10-11737-2010, 2010.

https://doi.org/10.5194/acp-2019-583
Preprint. Discussion started: 25 June 2019

471 Jacobson, M.Z. : Strong radiative heating due to the mixing state of black carbon in atmospheric aerosols,
472 Nature, 409(6821):695-697, 2001.
473 Johnson, K. S., Zuberi, B., Molina, L. T., Molina, M. J., Iedema, M. J., Cowin, J. P., Gaspar, D. J., Wang, C.,
474 and Laskin, A.: Processing of soot in an urban environment: Case study from the Mexico City
475 Metropolitan Area, Atmos. Chem. Phys.,5, 3033–3043, doi: 10.5194/acp-5-3033-2005, 2005.
476 Kulmala, M., Petaja, T., Monkkonen, P., Koponen, I.K., Dal Maso, M.,Aalto, P.P., Lehtinen, K.E.J., and
477 Kerminen, V.M. : On the growth of nucleation mode particles: source rates of condensable vapor in
478 polluted and clean environments, Atmos. Chem. Phys., 5, 409–416, doi: 10.5194/acp-5-409-2005, 2005.
479 Kuwata, M., Kondo, Y., Miyazaki, Y., Komazaki, Y., Kim, J. H.,Yum, S. S., Tanimoto, H., and Matsuedda,
480 H.: Cloud condensation nuclei activity at Jeju Island, Korea in spring 2005, Atmos. Chem. Phys., 8,
481 2933–2948,doi:10.5194/acp-8-2933-2008,2008.
482 Lee, A. K. Y., Willis, M. D., Healy, R. M., Onasch, T. B., and Abbatt, J. P. D.: Mixing state of carbonaceous
483 aerosol in an urban environment: single particle characterization using the soot particle aerosol mass
484 spectrometer (SP-AMS), Atmos. Chem. Phys., 15, 1823–1841, doi: 10.5194/acp-15-1823-2015, 2015.
485 Liu, D., Joshi, R., Wang, J., Yu, C., Allan, J. D., Coe, H., Flynn, M. J., Xie, C., Lee, J., Squires, F., Kotthaus,
486 S., Grimmond, S., Ge, X., Sun, Y., and Fu, P.: Contrasting physical properties of black carbon in urban
487 Beijing between winter and summer, Atmos. Chem. Phys. Discuss., doi: 10.5194/acp-2018-1142, in
488 review, 2018.
489 Liu, P. F., Zhao, C. S., Göbel, T., Hallbauer, E., Nowak, A., Ran,L., Xu, W. Y., Deng, Z. Z., Ma, N.,
490 Mildenberger, K., Henning,S., Stratmann, F., and Wiedensohler, A.: Hygroscopic properties of aerosol
491 particles at high relative humidity and their diurnal variations in the North China Plain, Atmos. Chem.
492 Phys., 3479–3494, doi:10.5194/acp-11-3479-2011, 2011.
493 Ma, Y., Brooks, S. D., Vidaurre, G., Khalizov, A. F., Wang, L., and Zhang, R.: Rapid modification of
494 cloud-nucleating ability of aerosols by biogenic emissions, Geophys. Res. Lett., 40, 6293–6297, doi:
495 10.1002/2013GL057895, 2013.

https://doi.org/10.5194/acp-2019-583
Preprint. Discussion started: 25 June 2019

496 Massling, A., Stock, M., and Wiedensohler, A.: Diurnal, weekly, and seasonal variation of hygroscopic
497 properties of submicrometer urban aerosol particles, Atmos. Environ., 39(21), 3911–3922, doi:
498 10.1016/j.atmosenv.2005.03.020, 2005.
499 Mei, F., Hayes, P. L., Ortega, A. M., Taylor, J. W., Allan, J. D., Gilman, J. B., Kuster, W. C., de Gouw, J. A.,
500 Jimenez, J. L., and Wang, J.: Droplet activation properties of organic aerosols observed at an urban site
501 during CalNex-LA, J. Geophys. Res., 118, 2903–2917, doi: 10.1002/jgrd.50285, 2013.
502 Mikhailov, E. F., Mironov, G. N., Pöhlker, C., Chi, X., Krüger, M. L., Shiraiwa, M., Förster, J. D., Pöschl,
503 U., Vlasenko, S. S., Ryshkevich, T. I., Weigand, M., Kilcoyne, A. L. D., and Andreae, M. O.: Chemical
504 composition, microstructure, and hygroscopic properties of aerosol particles at the Zotino Tall Tower
505 Observatory (ZOTTO), Siberia, during a summer campaign, At-mos. Chem. Phys., 15, 8847–8869,
506 doi:10.5194/acp-15-8847-2015, 2015.
507 Petters, M. D. and Kreidenweis, S. M.: A single parameter representation of hygroscopic growth and cloud
508 condensation nucleus activity, Atmos. Chem. Phys., 7, 1961–1971, doi: 10.5194/acp-7-1961-2007, 2007.
509 Ren, J. Y., Zhang, F., Wang, Y. Y., Collins, D., Fan, X. X., Jin, X. A., Xu, W. Q., Sun, Y. L., Cribb, M., and
510 Li, Z. Q.: Using different assumptions of aerosol mixing state and chemical composition to predict CCN
511 concentrations based on field measurements in urban Beijing, Atmos. Chem. Phys., 18, 6907–6921, doi:
512 10.5194/acp-18-6907-2018, 2018.
513 Saarnio, K., Frey, A., Niemi, J. V., Timonen, H., Rönkkö, T., Karjalainen, P., Vestenius, M., Teinilä, K.,
514 Pirjola, L., Niemelä, V.,Keskinen, J., Häyrinen, A., and Hillamo, R.: Chemical composition and size of
515 particles in emissions of coal-fired power plant with flue gas desulphurization, J. Aerosol Sci., 73, 14–26,
516 2014.
517 Sjogren, S., Gysel, M., Weingartner, E., Baltensperger, U., Cubison,M. J., Coe, H., Zardini, A. A., Marcolli,
518 C., Krieger, U. K., and Peter, T.: Hygroscopic growth and water uptake kinetics of two-phase aerosol
519 particles consisting of ammonium sulfate, adipic and humic acid mixtures, J. Aerosol Sci., 38, 157–171,
520 doi: 10.1016/j.jaerosci.2006.11.005, 2007.
521 Svenningsson, B., Rissler, J., Swietlicki, E., Mircea, M., Bilde, M.,Facchini, M. C., Decesari, S., Fuzzi, S.,
522 Zhou, J., Mønster, J., and Rosenørn, T.: Hygroscopic growth and critical supersaturations for mixed

https://doi.org/10.5194/acp-2019-583
Preprint. Discussion started: 25 June 2019

aerosol particles of inorganic and organic compounds of atmospheric relevance, Atmos. Chem. Phys., 6, 1937–1952, doi:10.5194/acp-6-1937-2006, 2006.

Sun, Y. L., Wang, Z. F., Du, W., Zhang, Q., Wang, Q. Q., Fu, P. Q., Pan, X. L., Li, J., Jayne, J., and Worsnop, D. R.: Long-term real-time measurements of aerosol particle composition in Beijing, China: Seasonal variations, meteorological effects, and source analysis, Atmos. Chem. Phys., 15, 10149–10165, doi: 10.5194/acp-15-10149-2015, 2015.

Sun, Y., Du, W., Fu, P., Wang, Q., Li, J., Ge, X., Zhang, Q., Zhu, C., Ren, L., Xu, W., Zhao, J., Han, T., Worsnop, D. R., and Wang, Z.: Primary and secondary aerosols in Beijing in winter: sources, variations and processes, Atmos. Chem. Phys., 16, 8309–8329, doi: 10.5194/acp-16-8309-2016, 2016.

Swietlicki, E., Hansson, H. C., HÄMeri, K., Svenningsson, B., Massling, A., McFiggans, G., McCurry, P. H., PetÄJÄ, T., Tunved, P., Gysel, M., Topping, D., Weingartner, E., Bal-tensperger, U., Rissler, J., Wiedensohler, A., and Kulmala, M.: Hygroscopic properties of submicrometer atmospheric aerosol particles measured with H-TDMA instruments in various environments - a review, Tellus B, 60, 432–469, doi: 10.1111/j.1600-0889.2008.00350.x, 2008.

Tan, H., Xu, H., Wan, Q., Li, F., Deng, X., Chan, P. W., Xia, D., and Yin, Y.: Design and application of an unattended multifunctional H-TDMA system, J. Atmos. Ocean. Tech., 30, 1136–1148, doi: 10.1175/JTECH-D-12-00129.1, 2013.

Turpin, B. J. and Lim, H. J.: Species contributions to PM2.5 mass concentrations: Revisiting common assumptions for estimating organic mass, Aerosol Sci. Tech., 35, 602–610, doi: 10.1080/02786820152051454, 2001.

Wang, J., Cubison, M. J., Aiken, A. C., Jimenez, J. L., and Collins, D. R.: The importance of aerosol mixing state and size-resolved composition on CCN concentration and the variation of the importance with atmospheric aging of aerosols, Atmos. Chem. Phys., 10, 7267–7283, doi:10.5194/acp-10-7267-2010, 2010.

Wang, J., Zhang, Q., Chen, M.-D., Collier, S., Zhou, S., Ge, X., Xu, J., Shi, J., Xie, C., Hu, J., Ge, S., Sun, Y., and Coe, H.: First chemical characterization of refractory black carbon aerosols and associated

https://doi.org/10.5194/acp-2019-583
Preprint. Discussion started: 25 June 2019

Atmospheric Chemistry and Physics Discussions

549 coatings over the Tibetan Plateau (4730 m a.s.l), Environ. Sci. Tech., 51, 14072,
550 doi:10.1021/acs.est.7b03973, 2017.
551 Wang, J. F., Liu, D. T., Ge, X. L., Wu, Y. Z., Shen, F. Z., Chen, M. D., Zhao, J., Xie, C. H., Wang, Q. Q.,
552 Xu, W. Q., Zhang, J., Hu, J. L., Allan, J., Joshi, R., Fu, P. Q., Coe, H., and Sun, Y. L.: Characterization of
553 black carbon-containing fine 10 particles in Beijing during wintertime, Atmos. Chem. Phys., 19, 447-458,
554 doi: 10.5194/acp-19-447-2019, 2019.
555 Wang, Q., Zhao, J., Du, W., Ana, G., Wang, Z., Sun, L., Wang, Y., Zhang, F., Li, Z., Ye, X., and Sun, Y.:
556 Characterization of submicron aerosols at a suburban site in central China, Atmos. Environ., 131, 115–
557 123, doi:10.1016/j.atmosenv.2016.01.054, 2016.
558 Wang, S. C. and Flagan, R. C.: Scanning Electrical Mobility Spectrometer, Aerosol Sci. Tech., 13, 230–240,
559 1990.
560 Wang, Y., Zhang, F., Li, Z., Tan, H., Xu, H., Ren, J., Zhao, J., Du, W., and Sun, Y.: Enhanced
561 hydrophobicity and volatility of submicron aerosols under severe emission control conditions in Beijing,
562 Atmos. Chem. Phys., 17, 5239–5251, doi: 10.5194/acp-17-5239-2017, 2017.
563 Wang Y., Li Z., Zhang Y., Du W., Zhang F., Tan H., Xu H., Fan T., Jin X., Fan X., Dong Z., Wang Q. and
564 Sun Y.: Characterization of aerosol hygroscopicity, mixing state, and CCN activity at a suburban site in
565 the central North China Plain, Atmos. Chem. Phys., 18, 11739-11752, doi: 10.5194/acp-18-11739-2018,
566 2018a.
567 Wang, Y., Z. Wu, N. Ma, Y. Wu, L. Zeng, C. Zhao, and A. Wiedensohler: Statistical analysis and
568 parameterization of the hygroscopic growth of the sub-micrometer urban background aerosol in Beijing,
569 Atmos. Environ., 175, 184-191, doi: 10.1016/j.atmosenv.2017.12.003, 2018b.
570 Wex, H., Petters, M. D., Carrico, C. M., Hallbauer, E., Massling,A., McMeeking, G. R., Poulain, L., Wu, Z.,
571 Kreidenweis, S. M.,and Stratmann, F. :Towards closing the gap between hygroscopic growth and
572 activation for secondary organic aerosol: Part 1—Evidence from measurements, Atmos. Chem. Phys., 9,
573 3987–3997, doi: 10.5194/acp-9-3987-2009, 2009

https://doi.org/10.5194/acp-2019-583
Preprint. Discussion started: 25 June 2019

574 Wu, Z., Hu, M., Lin, P., Liu, S., Wehner, B., and Wiedensohler, A.: Particle number size distribution in the
575 urban atmosphere of Beijing, China, Atmos. Environ., 42, 7967–7980, doi:
576 10.1016/j.atmosenv.2008.06.022, 2008.
577 Wu, Z. J., Poulain, L., Henning, S., Dieckmann, K., Birmili, W.,Merkel, M., van Pinxteren, D., Spindler, G.,
578 Müller, K., Strat-mann, F., Herrmann, H., and Wiedensohler, A.: Relating particle hygroscopicity and
579 CCN activity to chemical composition during the HCCT-2010field campaign, Atmos. Chem. Phys., 13,
580 7983–7996, doi: 10.5194/acp-13-7983-2013, 2013.
581 Wu, Z. J., Zheng, J., Shang, D. J., Du, Z. F., Wu, Y. S., Zeng, L. M., Wiedensohler, A., and Hu, M.: Particle
582 hygroscopicity and its link to chemical composition in the urban atmosphere of Beijing, China, during
583 summertime, Atmos. Chem. Phys., 16, 1123–1138, doi: 10.5194/acp-16-1123-2016, 2016.
584 Xu, W. Q., Sun, Y. L., Chen, C., Du, W., Han, T. T., Wang, Q. Q.,Fu, P. Q., Wang, Z. F., Zhao, X. J., Zhou,
585 L. B., Ji, D. S., Wang,P. C., and Worsnop, D. R.: Aerosol composition, oxidation properties, and sources
586 in Beijing: results from the 2014 Asia-Pacific Economic Cooperation summit study, Atmos. Chem. Phys.,
587 15,13681–13698, doi:10.5194/acp-15-13681-2015, 2015.
588 Ye, X., Tang, C., Yin, Z., Chen, J., Ma, Z., Kong, L., Yang, X., Gao, W., and Geng, F.: Hygroscopic growth
589 of urban aerosol particles during the 2009 Mirage-Shanghai Campaign, Atmos. Environ., 64, 263–269,
590 doi:10.1016/j.atmosenv.2012.09.064, 2013.
591 Zardini, A. A., Sjogren, S., Marcolli, C., Krieger, U. K., Gysel,M., Weingartner, E., Baltensperger, U., and
592 Peter, T.: A combined particle trap/HTDMA hygroscopicity study of mixed in-organic/organic aerosol
593 particles, Atmos. Chem. Phys., 8, 5589–5601, doi:10.5194/acp-8-5589-2008, 2008
594 Zhang, F., Li, Y., Li, Z., Sun, L., Li, R., Zhao, C., Wang, P., Sun, Y., Liu, X., Li, J., Li, P., Ren, G., and Fan,
595 T.: Aerosol hygroscopicity and cloud condensation nuclei activity during the AC3Exp campaign:
596 Implications for cloud condensation nuclei parameterization, Atmos. Chem. Phys., 14, 13423–13437, doi:
597 10.5194/acp-14-13423-2014, 2014.
598 Zhang, F., Li, Z., Li, Y., Sun, Y., Wang, Z., Li, P., Sun, L., Wang, P., Cribb, M., Zhao, C., Fan, T., Yang, X.,
599 and Wang, Q.: Impacts of organic aerosols and its oxidation level on CCN activity from measurement at a
600 suburban site in China, Atmos. Chem. Phys., 16, 5413–5425, doi: 10.5194/acp-16-5413-2016, 2016.

https://doi.org/10.5194/acp-2019-583
Preprint. Discussion started: 25 June 2019

Atmospheric Chemistry and Physics Discussions

601 Zhang, F., Wang, Y., Peng, J., Ren, J., Zhang, R., Sun, Y., Collin, D., Yang, X., and Li, Z.: Uncertainty in
602 predicting CCN activity of aged and primary aerosols, J. Geophys. Res.-Atmos., 122, 11723–11736, doi:
603 10.1002/2017JD027058, 2017.
604 Zhang, R., Khalizov, A. F., Pagels, J., Zhang, D., Xue, H., and McMurry, P. H.: Variability in morphology,
605 hygroscopicity, and op-tical properties of soot aerosols during atmospheric processing, PNAS, 105(30),
606 10291–10296, doi:10.1073/pnas.0804860105,2008.
607 Zhang, Q., Stanier, C. O., Canagaratna, M. R., Jayne, J. T., Worsnop, D. R., Pandis, S. N., & Jimenez, J. L. :
608 Insights into the chemistry of new particle formation and growth events in Pittsburgh based on aerosol
609 mass spectrometry, Environmental Science & Technology, 38(18), 4797–4809, doi: 10.1021/es035417u,
610 2004.
611 Zhao, J., Du, W., Zhang, Y., Wang, Q., Chen, C., Xu, W., Han, T., Wang, Y., Fu, P., Wang, Z., Li, Z., and
612 Sun, Y.: Insights into aerosol chemistry during the 2015 China Victory Day parade: results from
613 simultaneous measurements at ground level and 260 m in Beijing, Atmos. Chem. Phys., 17, 3215–3232,
614 doi: 10.5194/acp-17-3215-2017, 2017.